Uniaxial-Stress Effects on the Emission Bands of KI:Tl Phosphor

T. SHIMADA AND M. ISHIGURO
Institute of Scientific and Industrial Research, Osaka University, Suita, Osaka, Japan
(Received 17 December 1968)

The effect of uniaxial stress on the emissions of KI:Tl phosphor has been measured over the temperature range from 2 to 70°K. A discussion is given of the stress-induced dichroism resulting from the perturbation of excited states by the uniaxial stress. With plausible assumptions, coupling constants between the p electrons and the E_g or T_{2g} lattice distortion are estimated. The coupling constants thus obtained are consistent with the point-charge model. The stress effects below 35°K are very complex, owing to the correlation of the polarization of luminescence.

I. INTRODUCTION

IN 1953 Yuster and Delbecq[1] found triplet structure in the C band of KI:Tl. More recently, a systematic study of the absorption spectra for various combinations of host alkali halides and impurity ions was made by Fukuda *et al.*[2] They found that in alkali halide–heavy-metal phosphors, the A and C bands have doublet and triplet structures, respectively. Toyozawa and Inoue[3] explained this structure in terms of the dynamical Jahn-Teller effect, and estimated the coupling constants between the p electrons and the lattice distortions. Recently, Cho[4] carried out a more general analysis for the line shape in terms of various combinations of the coupling constants between the p electron and the A_{1g}-, E_g-, and T_{2g}-mode lattice distortions. In connection with the electron-lattice interaction, it is very interesting to note that some of these emission bands are partially polarized when the phosphor is excited by plane-polarized light in a suitable absorption band at low temperature.[5] Fukuda *et al.*[6] made a systematic investigation of the correlation of the polarization in KBr doped with Ga, In, Tl, and Pb, and concluded that the tetragonal Jahn-Teller distortion alone determines the stable lattice configuration of the excited states relative to the A and C bands.

The measurement of the stress effects on the absorption and emission spectra is a useful method for the investigation of the electron-lattice interactions in these phosphors. The application of uniaxial stress (non-totally-symmetric distortion) will give quantitative information on the electron-lattice interaction. In the present work, we studied the effect of uniaxial stress on the emission bands of KI:Tl. At 12°K, the KI:Tl phosphor shows two emission bands, peaking at 336 and 430 mμ, upon irradiation in the A absorption band (281 mμ); and five emission bands, peaking at 272, 289, 304, 336, and 430 mμ, upon irradiation in the C absorption band (233 mμ).[7] The electronic states corresponding to the emission bands were investigated by Johnson and Williams,[8] Kamimura and Sugano,[9] Illingworth,[10] Edgerton,[11] and many other investigators. The result of their investigations gives the assignment for the emission bands as shown in Table I. The assignment of the emission bands of KI:Tl is fairly well clarified. That is one of the reasons why we first chose this crystal for the present study. The stress-splitting energy induced by an applied [001] stress within the elastic limit is very small and of the order of 10^{-3} eV, so that the peak shift of the emission band is not large enough to be measured quantitatively. However, we can get the stress-splitting energy accurately through the observation of the stress-induced dichroism induced by the population difference between the relaxed excited states (p-like states) in the E_g subspace of lattice distortion. From the stress-splitting energy mentioned above, we can estimate the coupling constant between the p electron and the tetragonal-lattice distortion. A large dichroism is also induced by the rotation of the transition moment due to the mixing of the eigenstates. Such a mixing can be produced by the trigonal-lattice distortion. Thus, the coupling con-

TABLE I. The assignments for the emission bands of KI:Tl phosphor.[a]

Emission band (mμ)	Excited state	Ground state
272	$^1T_{1u}$	$^1A_{1g}$
289	^3E_u and/or $^3T_{2u}$	$^1A_{1g}$
304	$^3T_{2u}$	$^1A_{1g}$
336	$^3T_{1u}$	$^1A_{1g}$
430	$^3T_{1u}$?, $^3A_{1u}$? or other states	$^1A_{1g}$

[a] See Refs. 8–11.

[1] P. H. Yuster and C. J. Delbecq, J. Chem. Phys. **21**, 892 (1953).
[2] A. Fukuda, K. Inohara, and R. Onaka, J. Phys. Soc. Japan **19**, 1274 (1964); A. Fukuda, Sci. Light (Tokyo) **13**, 64 (1964); R. Onaka, A. Fukuda, and T. Mabuchi, J. Phys. Soc. Japan **20**, 466 (1965); A. Fukuda and S. Makishima, Phys. Letters **24A**, 267 (1967).
[3] Y. Toyozawa and M. Inoue, J. Phys. Soc. Japan **21**, 1663 (1966).
[4] K. Cho, Technical Report of ISSP University of Tokyo, Ser. A No. 351, 1969 (unpublished).
[5] C. C. Klick and W. D. Compton, J. Phys. Chem. Solids **7**, 170 (1958).
[6] A. Fukuda, S. Makishima, T. Mabuchi, and R. Onaka, J. Phys. Chem. Solids **28**, 1763 (1967).
[7] R. Edgerton and K. Teegarden, Phys. Rev. **129**, 169 (1963); **136**, A1091 (1964).
[8] P. D. Johnson and F. E. Williams, J. Chem. Phys. **20**, 124 (1952).
[9] H. Kamimura and S. Sugano, J. Phys. Soc. Japan **14**, 1612 (1959).
[10] R. Illingworth, Phys. Rev. **136**, A508 (1964).
[11] R. Edgerton, Phys. Rev. **138**, A85 (1965).

stant between the p electron and the trigonal-lattice distortion is estimated from the effect of the [110] uniaxial stress.

We also investigate the stress effect on the correlation of polarization described above, the relation between the stress effect and the photon energy of the exciting light, and an anomalous stress effect at extreme low temperatures.

II. EXPERIMENTAL PROCEDURE

Figure 1 shows the experimental arrangement used in the investigation of the effect of uniaxial stress. The light source used was a 500-W xenon lamp. The exciting light monochromated by a prism monochromator was focused on to the sample. A polarizer was inserted between the monochromator and the Dewar. The emissions from the specimen were detected from a direction perpendicular to the incident light, by means of the arrangement consisted of a quartz lens, an analyzer, a single-prism spectrometer, and a photomultiplier. The polarization caused by the measuring system was cancelled with the pile of plates made of fused quartz. The uniaxial stress was applied at right angle to the exciting light beam and to the emitted light beam passing through the measuring arrangement. A schematic drawing of the operation is shown in Fig. 2. The sample cell, consisting of a piston and a holder, is made of phosphor bronze (Fig. 3). Thin aluminum foils were inserted between the sample and the holder, and between the sample and the piston, as buffers. The stress was transmitted to the sample cell by a stainless-steel rod and a lever; the lever was pulled with a spring balance for the measurement of the magnitude of the stress. The stress was applied intermittently with a 4-rpm motor. The spectrometer for the emissions was scanned through the whole wavelength range of the emission spectra in synchronism with a recorder. This modulation method not only provides highly sensitive and rapid measurements, but also enables us to look directly at the data recorded and eliminates the error due to the gradual variation of sensitivity and zero level. The sample cell was held in a cryostat made of fused quartz and cooled with liquid helium or its vapor.

The maximum uniaxial stress within the elastic limit is 3 kg/mm² for the [001] direction and 6 kg/mm² for the [110] direction at 2°K, and 1.5 kg/mm² for the [001] direction and 3 kg/mm² for the [110] direction at 77°K. The temperature of the sample was measured with a carbon resistor (2–10°K) and a Pt-Au:Co or chromel-Au:Co thermocouple (above 4°K). The samples of KI:Tl were obtained by cleaving and/or polishing single crystals grown by the Kyropolous method, adding about 0.005-mole% TlI to the melt. Their dimensions were 4.5×1.5×6.0 mm.

The reproducibility of the stress spectra was kept within ±0.5% in terms of the signal intensity for the same sample; but between different samples, there were the maximum fluctuations of about ±20%.

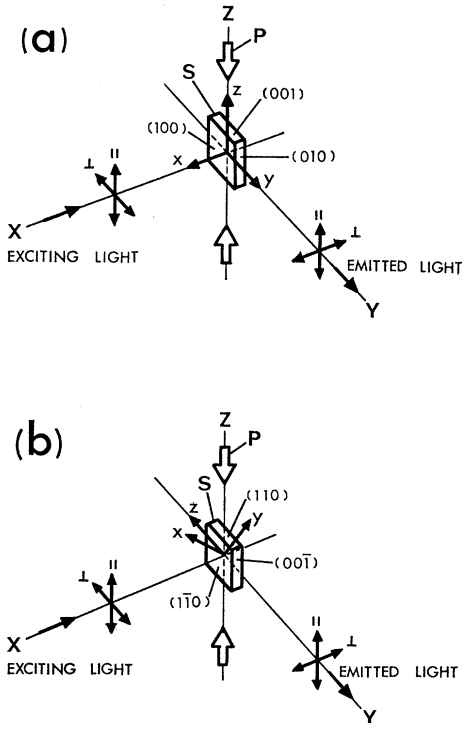

FIG. 1. Arrangement of optical systems and crystal axes. (a) Arrangement for ⟨001⟩ stress. (b) Arrangement for ⟨110⟩ stress. X, Y, Z are axes of optical system, x, y, z are crystal axes, P is the direction of uniaxial stress, and S is a sample.

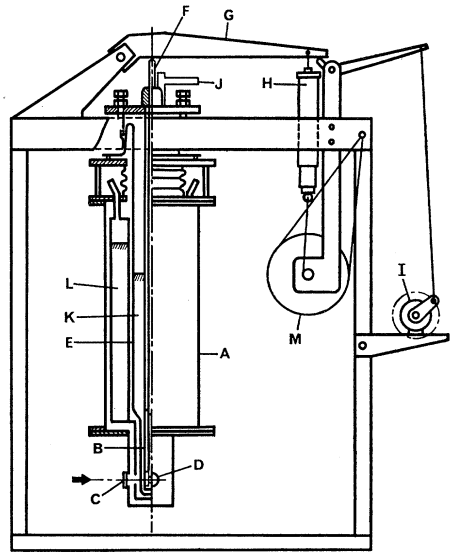

FIG. 2. Schematic drawing of cryostat and its location: A is the cryostat, B is the sample cell, C is the fused-quartz widow for excitation, D is the window for measurement of luminescence, E is the fused-quartz vessel, F is the stainless-steel rod, G is the lever, H is the spring balance, I is the drive motor (4 rpm) for intermittent application of the stress, J is the helium-gas outlet, K is liquid helium, L is liquid nitrogen, and M is the brake.

III. EXPERIMENTAL RESULTS AND DISCUSSION

The observation of the stress effects on the emissions was made by measuring the components of the emission polarized parallel or perpendicular to the stress under irradiation by light polarized parallel or perpendicular to the stress. We refer to these measurements as (∥,∥), (∥,⊥), (⊥,∥), and (⊥,⊥) hereafter. The first and second symbols in each bracket show the directions of polarization of the exciting and the emitted light, respectively, with respect to the stress. Each polarized component of the emission is expressed as $I_{\parallel}^{0}$ and $I_{\perp}^{0}$ in the case without stress, and as $I_{\parallel}$ and $I_{\perp}$ in the case with stesss, and the differences between the two cases are expressed as $\Delta I_{\parallel}$ and $\Delta I_{\perp}$. The examples of the recorded emission spectra modulated by the periodic stress are shown in Figs. 4 and 5.

A. Case of ⟨001⟩ Uniaxial Stress

1. Experimental Results

This phosphor shows a large stress-induced dichroism in the 272- and 336-mμ emission bands when excited in the *C* band, and in the 336-mμ emission band when excited in the *A* band. A slight stress effect appears on the 430-mμ emission band, but no stress effect appears on the 289-mμ emission band within the accuracy of our measurements. It seems that no stress effect appears on the 304-mμ emission band either, though there is an uncertainty because of its very weak intensity. In Figs. 4 and 5, the periodic variation in the spectrum curve indicates the stress effect, and the direction of an arrow indicates the direction of variation of the emission spectrum due to the stress. For example, it is shown in Fig. 5 that the (∥,∥) component of the 336-mμ emission band excited in the *C* absoprtion band increases by applied ⟨001⟩ stress. It is evident that there is a large intensity change but no shape variation and no peak shift. Here, we will attend to 336- and 272-mμ emission bands which show a large stress-induced dichroism. In the 336-mμ band, the ∥ component (emissions polarized parallel to the stress) increases and the ⊥ component derceases as stress is applied; but in the 272-mμ band the situation is just the opposite. In addition, the total intensity of the polarized components of the emissions is kept constant regardless of the applied stress. Figure 6 shows the temperature dependence of the stress effect $\Delta I_{\parallel(\perp)}/I^{0}$ [where $I^{0}=\frac{1}{3}(I_{\parallel}^{0}+2I_{\perp}^{0})$] and of the degree of polarization $P[=(I_{\parallel}^{0}-I_{\perp}^{0})/(I_{\parallel}^{0}+I_{\perp}^{0})]$ of the 336-mμ band produced by irradiation in the center of the *A* band. Plots of $\Delta I_{\parallel}$ and $\Delta I_{\perp}$ of the 336-mμ band versus applied stress are shown in Fig. 7. They are nearly in proportion to the stress over the range of applied stress, 0–2 kg/mm². It is interesting to note that $\Delta I_{\parallel(\perp)}/I^{0}$ is independent of the direction of polarization of the exciting light above 35°K, but is not below 35°K, and *P* falls abruptly to zero at 30°K. Figures 8 and 9 show

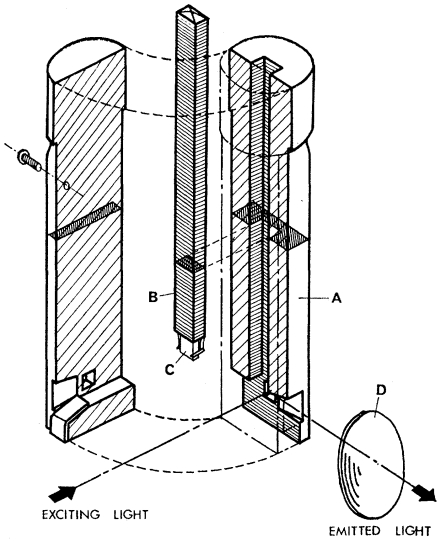

FIG. 3. Sample cell made of phosphor bronze. A is the holder, B is the piston, C is the sample, and D is the lens.

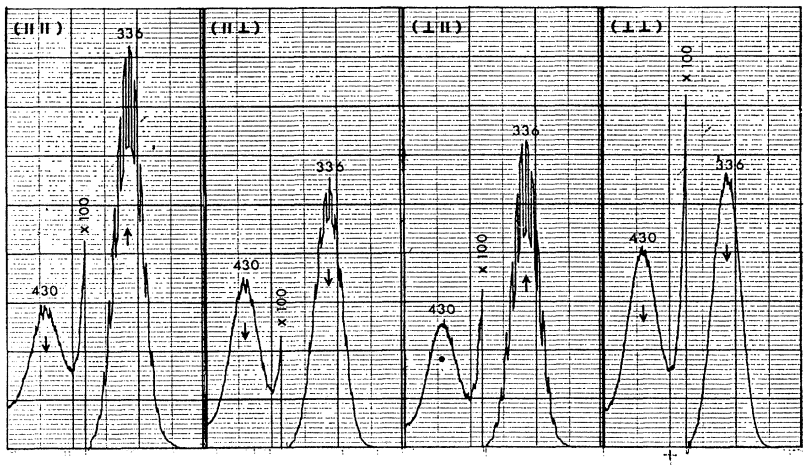

FIG. 4. Emission spectra modulated by periodic ⟨001⟩ stress (excited in the *A* absorption band at 2°K). The applied ⟨001⟩ stress is 2 kg/mm².

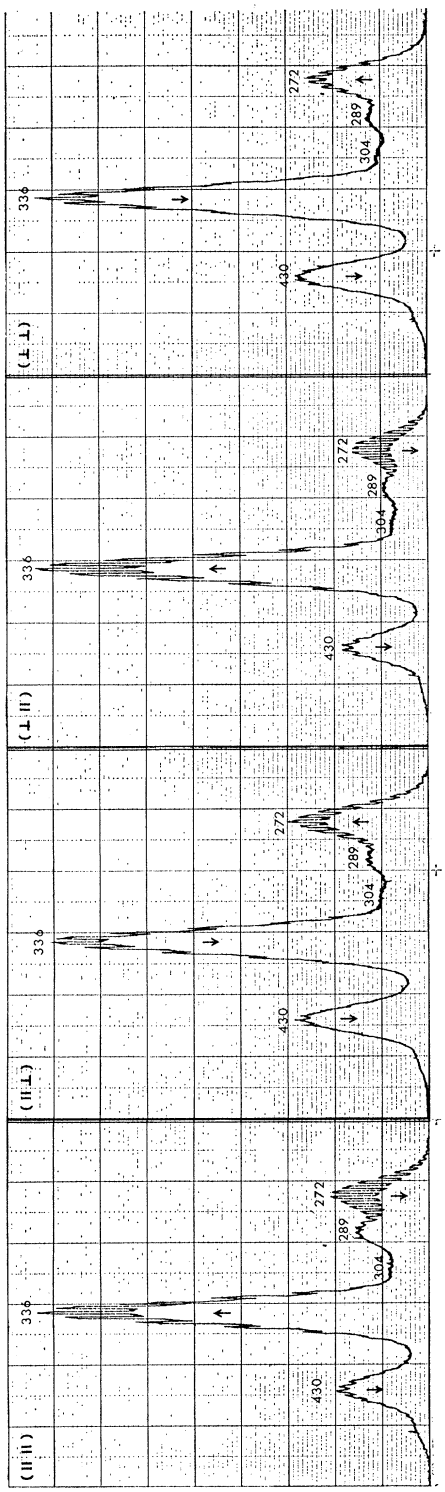

FIG. 5. Emission spectra modulated by periodic ⟨001⟩ stress (excited in the C absorption band at 2°K). The applied ⟨001⟩ stress is 2 kg/mm².

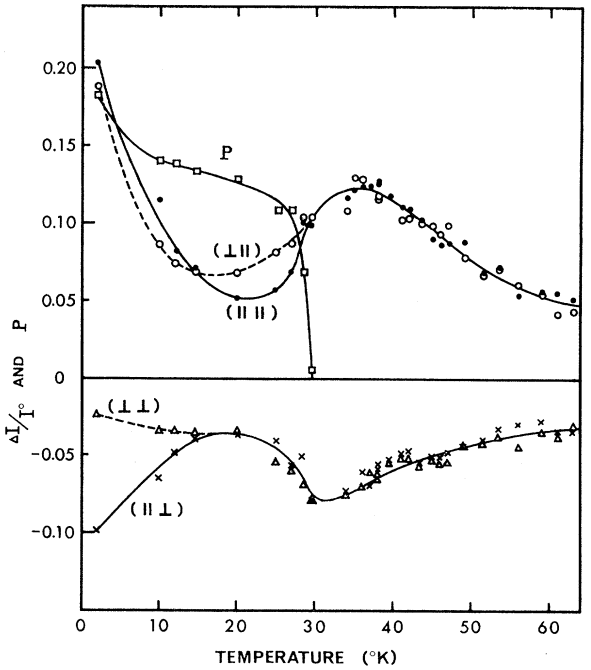

FIG. 6. Temperature dependence of the stress effect on the 336-mμ emission band (excited in the A absorption band) and the correlation of the polarization P. The applied ⟨001⟩ stress is 1 kg/mm².

the stress effect on P as a function of the photon energy of the exciting light. The remarkable point in these figures is that the applied stress causes a variation of the polarization independent of the photon energy of the exciting light.

2. *Origin of Stress-Induced Dichroism*

The large dichroism on the 336- and 272-mμ bands induced by a uniaxial stress of the order of 2 kg/mm² cannot be explained by the variation of the oscillator strength. On the other hand, there is a possibility that

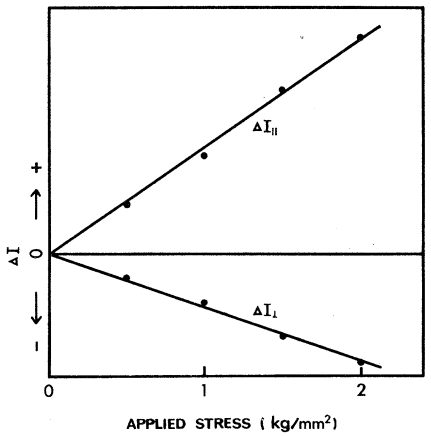

FIG. 7. Increment of the 336-mμ emission band versus applied ⟨001⟩ stress at 35°K.

it might be a noncubic center such as an off-center atom.[12] But, considering various experimental results, an interpretation on the basis of a cubic center displaying the Jahn-Teller effect[9,13–16] seems to be most natural. The splitting of the excited states (splitting between the three minimum points in E_g subspace) due to the applied stress will cause a population difference between those states. Since the directions of the transition moment between each split excited state and the totally symmetric nondegenerate ground state are specific for the direction of the stress. The intensity of the luminescence will depend on its polarization with respect to the direction of the stress—in other words, there appears a stress-induced dichroism. Uniaxial stress applied in a ⟨001⟩ direction gives the Q_1- and Q_3-mode distortion (cf. Sec. IV A) to the phosphor. The Q_1 distortion is not of interest, but the tetragonal distortion Q_3 gives the above dichroism. From the dichroic spectrum, we can see that the ratio of the increment of the $\parallel$ component of the emissions to that of the $\perp$ component is $2:-1$ for the 336-mμ band, and $-2:1$ for the 272-mμ band; we can thus confirm that the initial state of the 336-mμ band is the $^3T_{1u}$, and that of the 272-mμ band is the $^1T_{1u}$, by referring to the population effect mentioned above, the energy-level diagram in the ionic model, and the electron-lattice interaction matrix (Sec. IV). The Q_3 distortion splits the triply degenerate state $^3T_{1u}$ into the nondegenerate and doubly degenerate states. The energy of the nondegenerate state is lower than that of the doubly degenerate state. The $^1T_{1u}$ state also splits into the nondegenerate and doubly degenerate states, but in the reverse order. The above situation leads us to the conclusion that the coupling constant b between the p electron and the tetragonal-lattice distortion is negative.

3. *Temperature Dependence of Stress Effects and Stress-Induced Splitting Energy ΔE*

It is considered that, above 35°K, thermal equilibrium exists between three minimum points of electronic state $^3T_{1u}$ in the subspace of E_g-mode lattice distortion, because the stress effect is independent of the polarization of the exciting light, the ratio of $\Delta I_{\parallel}/I^0$ to $\Delta I_{\perp}/I^0$ is $2:-1$, and the correlation of the polarization is equal to zero as shown in Fig. 6. At lower temperatures, however, thermal equilibrium will not exist, because of the potential barrier between minumum points of adiabatic potentials for the electronic states $^3T_{1u}$ in the subspace of E_g-mode lattice distortions. The appearance of the correlation of the polarization of luminescence, and of the stress effects dependent on the polarization

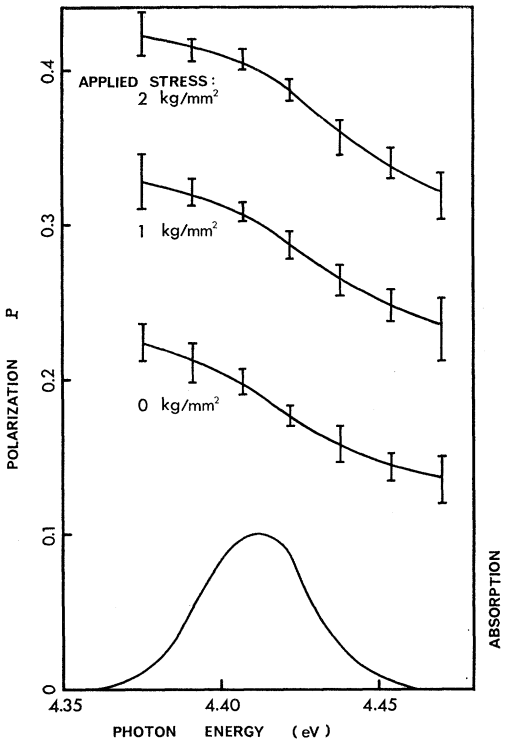

FIG. 8. Stress effect on the correlation of the polarization P (between A absorption band and 336-mμ emission band) measured at 2°K. Absorption spectrum is shown in the lower part of the figure.

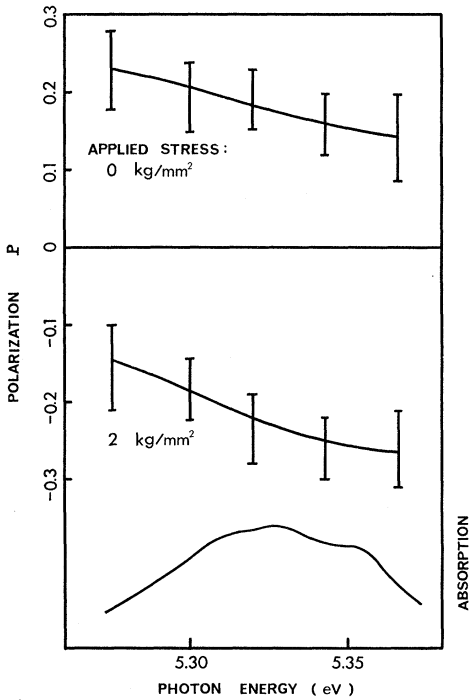

FIG. 9. Stress effect on the correlation of polarization P (between C absorption band and 272-mμ emission band) measured at 2°K. Absorption spectrum is shown in the lower part of the figure.

[12] H. Kanzaki, Proc. Phys. Soc. Japan **21**, 707 (1966).
[13] H. A. Jahn and E. Teller, Proc. Roy. Soc. (London) **A161**, 220 (1937).
[14] H. A. Jahn, Proc. Roy. Soc. (London) **A164**, 117 (1938).
[15] J. H. Van Vleck, J. Chem. Phys. **7**, 72 (1939).
[16] U. Öpik and M. H. Pryce, Proc. Roy. Soc. (London) **A238**, 425 (1957).

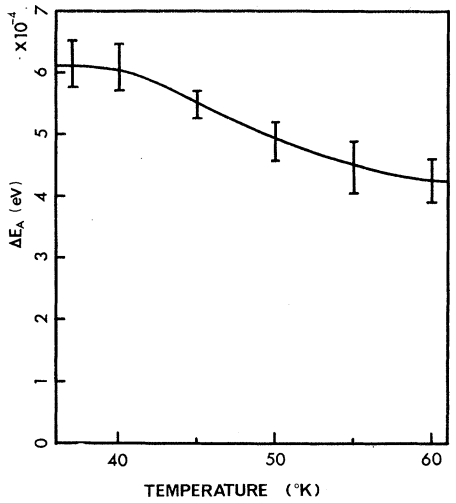

FIG. 10. Temperature dependence of the stress-splitting energy ΔE_A. The applied ⟨001⟩ stress is 1 kg/mm².

SYSTEM	EFFECT ON 272mμ BAND	EFFECT ON 336mμ BAND	EFFECT ON 430mμ BAND
(∥ ∥)	↓	↑ ⇡	↓ ⇣
(∥ ⊥)	↓	↑ ⇡	• ⇡
(⊥ ∥)	↓	↑ ⇡	↓ ⇣
(⊥ ⊥)	↓	↑ ⇡	↓ ⇡

⇡ : A BAND EXCITATION, ⇡ : C BAND EXCITATION

FIG. 11. Qualitative description of ⟨110⟩ stress effects on emission bands. The length of the arrows shows the amount of the change in the intensity of emission, and their upward and downward directions indicate an increase and decrease of the emission intensity, respectively.

of exciting light, below 30°K seems to support this situation. Below 30°K, however, the situation is complex and closely connected with the correlation of the polarization of luminescence. The stress effect on the 336-mμ emission band depends on the direction of polarization of exciting A light, but when the emission band was produced by C-light irradiation (transition from the $^1T_{1u}$ to the $^3T_{1u}$ is a phonon process), the stress effect was independent of the direction of polarization of exciting C light. These experimental facts are consistent with the above description. It is curious that the stress effect increases again after passing through the minimum point at about 20°K. This large stress-induced dichroism at extreme low temperatures suggests that some processes such as tunneling or mixing of electronic states by lattice vibration belonging to the T_{2g} symmetry are involved. From the fact that the process occurs at extreme low temperatures, the latter explanation is not adequate for the present case. On the other hand, the effect might be related to an off-center atom, but at present we have no experimental data bearing on this possibility. In the non-thermal-equilibrium case, the stress effect for relaxation processes from the optically excited state to the relaxed excited state must also be considered. However, the fact that the application of the stress increases the value of the polarization P independently of the exciting photon energy suggests that the stress effect will be rather small for the relaxation process, but rather large for the transition between minimum points of adiabatic potentials. The situation below 35°K is very complex, as mentioned above; but above this temperature, thermal equilibrium holds approximately, and therefore the stress-splitting energy ΔE_A may be obtained from a Boltzmann factor (see Fig. 10). The decrease of ΔE_A with temperature seems to be due to thermal quenching of the 336-mμ band, resulting in an increase of the 430-mμ band. ΔE_A was estimated at the lowest temperature in thermal equilibrium range, and the value thus obtained is as follows:

$$\Delta E_A = 6.2\times 10^{-4} \text{ eV/kg/mm}^2.$$

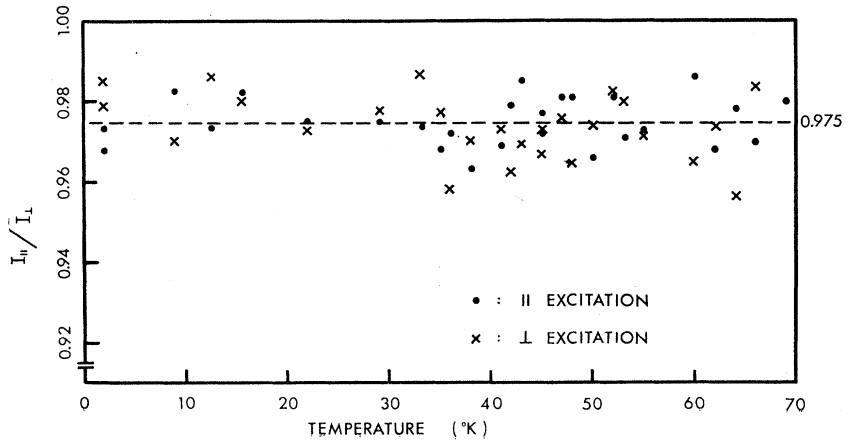

FIG. 12. Temperature dependence of the stress effect on the 336-mμ band under applied ⟨110⟩ stress. The applied ⟨110⟩ stress is 1.66 kg/mm².

B. Case of ⟨110⟩ Uniaxial Stress

1. Experimental Results

In this case, Q_1, Q_3, and Q_6 distortions arise, rather than just Q_1 and Q_3 as in the earlier case (Sec. IV B). Here we can get information about the Q_6 mode, using the result obtained in the case of ⟨001⟩ stress. Experimental results show that both the $\parallel$ and $\perp$ components of the 336-mμ emission band produced by excitation in the A or C absorption bands increase with applied stress; but for the 272-mμ emission band produced by excitation in the C absorption band, they decrease.

A different type of stress effect appears on the 430-mμ emission band. But no stress effect appears in the 289-mμ band, nor (probably) in the 304-mμ band. These cases are shown in Fig. 11. The length of the arrows shows approximately the amount of change in the intensity of emissions, and their upward and downward directions indicate an increase and decrease of the emission intensity, respectively.

The stress effects on the 336-mμ emission band excited in the A band were measured at various temperatures, and the data were treated by the following method. Since the Q_3 distortion gives an equal stress effect to the $\parallel$ and $\perp$ components of the emission, the effect of the Q_6 distortion determines the value of r as

$$r=I_{\parallel}/I_{\perp}, \tag{1}$$

where $I_{\parallel}$ and $I_{\perp}$ are the intensities of the emissions polarized parallel and perpendicular to the applied stress, respectively. A plot of r versus temperature is shown in Fig. 12. It is found that the stress effect of the Q_6 distortion is independent of temperature, and therefore will not be involved in the population effect. The mean observed value of r is about 0.975 ($P=1.66$ kg/mm^2). The origin of this stress-induced dichroism is the rotation of the transition moments caused by the Q_6 distortion, which will be discussed in Sec. IV.

IV. COUPLING CONSTANTS

The Hamiltonian for the system under the applied external force can be shown as follows:

$$\mathcal{H}=\mathcal{H}_E(\mathbf{r})+\mathcal{H}_{so}(\mathbf{r},\mathbf{s}) +\sum_{i=1}^{6}[(P_i^2/2M_i)+\tfrac{1}{2}K_iQ_i^2+V_i(\mathbf{r})Q_i-F_iQ_i], \tag{2}$$

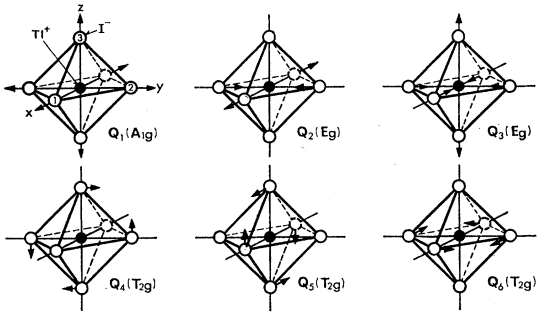

FIG. 13. The even normal modes of an octahedral quasimolecule, type XY_6.

where the first term is the kinetic and electrostatic energy of the electrons; the second is the spin-orbit interaction energy; the third and fourth are, respectively, the kinetic and the elastic energy of each mode of distortion [$A_{1g}(Q_1)$, $E_g(Q_2,Q_3)$, and $T_{2g}(Q_4,Q_5,Q_6)$ (Fig. 13)]; the fifth is the linear part of the electron-lattice interaction energy; and the sixth is the energy due to the external force. Here we are interested only in the part concerned with the Jahn-Teller effect and the stress effect of Eq. (2). Within the framework of the Franck-Condon approximation, it is given as

$$\mathcal{H}'=\mathcal{H}^{(1)}+\mathcal{H}^{(2)}+\mathcal{H}^{(3)} =\sum_{i=1}^{6}[\tfrac{1}{2}K_iQ_i^2+V_i(\mathbf{r})Q_i-F_iQ_i]. \tag{3}$$

The eigenstates of the s-p electronic configuration were given by Toyozawa and Inoue[3] as follows:

$$|A^k\rangle=-t|{}^1T_{1u}{}^k\rangle+(1-t^2)^{1/2}|{}^3T_{1u}{}^k\rangle, \quad k=x,y,z \tag{4a}$$

$$|C^k\rangle=(1-t^2)^{1/2}|{}^1T_{1u}{}^k\rangle+t|{}^3T_{1u}{}^k\rangle, \quad k=x,y,z \tag{4b}$$

where A^k and C^k are the excited states of the A (336 mμ) and C (272 mμ) emission bands, ${}^1T_{1u}{}^k$ and ${}^3T_{1u}{}^k$ are the singlet and triplet states, respectively, and t is a mixing parameter due to the spin-orbit interaction. Thus, the interaction matrix corresponding to $\mathcal{H}^{(2)}$ is given as

$$\langle\psi^k|\mathcal{H}^{(2)}|\psi^l\rangle=\begin{bmatrix}\beta\{Q_2-(1/\sqrt{3})Q_3\}, & \gamma Q_6, & \gamma Q_5,\\ \gamma Q_6, & \beta[-Q_2-(1/\sqrt{3})Q_3], & \gamma Q_4,\\ \gamma Q_5, & \gamma Q_4, & \beta(2/\sqrt{3})Q_3\end{bmatrix}, \tag{5}$$

where ψ^k is A^k or C^k. For the A state,

$$\beta=-\tfrac{1}{2}(1-3t^2)b, \tag{6a}$$

$$\gamma=-\tfrac{1}{2}(1-3t^2)c, \tag{6b}$$

and for the C state,

$$\beta=(1-\tfrac{3}{2}t^2)b, \tag{6c}$$

$$\gamma=(1-\tfrac{3}{2}t^2)c. \tag{6d}$$

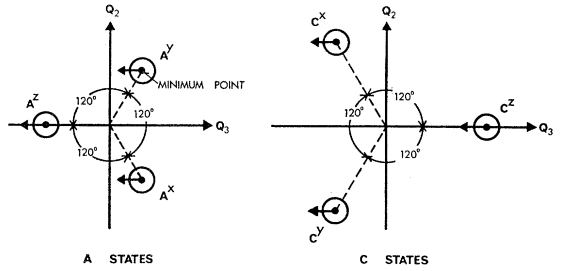

FIG. 14. Stress effect on minimum points of adiabatic potentials for the A and C states in E_g subspace.

The coupling constants b and c are defined by

$$b=\langle p_x|V_2(\mathbf{r})|p_x\rangle=\langle p_x|k(E_g)(x^2-y^2)|p_x\rangle, \quad (7a)$$

$$c=\langle p_y|V_4(\mathbf{r})|p_z\rangle=\langle p_y|k(T_{2g})(yz)|p_z\rangle. \quad (7b)$$

A. Coupling Constant for E_g Mode

A uniaxial stress applied in a ⟨001⟩ direction is decomposed into the various symmetry components as follows[17]:

$$P_1=\tfrac{1}{3}P \quad (A_{1g}), \quad (8a)$$

$$P_3=\tfrac{2}{3}P \quad (E_g), \quad (8b)$$

where the subscript on the P corresponds to the Q's in Fig. 13. The P_1 is a totally symmetric distortion and is not of interest to us. Thus, we will discuss the electron-lattice interaction in the E_g subspace, neglecting the dynamical effects of lattice vibration. Fukuda's experimental results show that the stable Jahn-Teller distortion is determined only in the E_g-mode subspace.

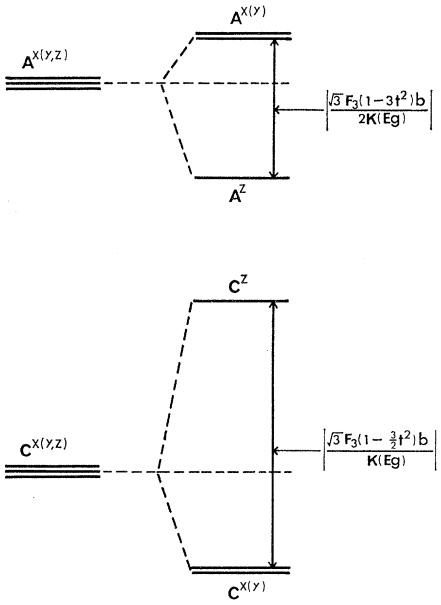

FIG. 15. Energy levels at the three minimum points of the A and C states under ⟨001⟩ stress.

[17] C. H. Henry, S. E. Schnatterly, and C. P. Slichter, Phys. Rev. **137**, A583 (1965).

Since the T_{2g} distortion need not be taken into consideration, we have

$$Q_4=Q_5=Q_6=0, \quad (9)$$

and the matrix (5) is diagonalized. Therefore the minimum eigenvalues in the E_g subspace can easily be obtained, and the energy differences ΔE between these minimum points are given by

$$\Delta E={}^0E^{x(y)}-{}^0E^z=-\sqrt{3}\beta F_3/K(E_g), \quad (10)$$

where ${}^0E^{x(y,z)}$ is the energy at the minimum points of each state $\psi^{x(y,z)}$ in the E_g subspace. Using Eqs. (6a)–(6d), we can get the splitting energies in the A and C states as

$$\Delta E_A={}^0E_A{}^{x(y)}-{}^0E_A{}^z=\sqrt{3}F_3(1-3t^2)b/2K(E_g), \quad (11a)$$

$$\Delta E_C={}^0E_C{}^{x(y)}-{}^0E_C{}^z=-\sqrt{3}F_3(1-\tfrac{3}{2}t^2)b/K(E_g). \quad (11b)$$

The above situation is shown in Figs. 14 and 15. The splitting of the A and C states are in opposite directions and are not equal in magnitude. These results are consistent with the experimental observations.

In Eq. (11a), ΔE_A is given in Sec. III A 3, and F_3 and $K(E_g)$ can be estimated, with the use of the definition of the Q_3 expressed by $X_1=Y_2=-(1/2\sqrt{3})Q_3$ and $Z_3=(1/\sqrt{3})Q_3$ (where X_1, Y_2, and Z_3 are the displacements of the first, second, and third ligand ions, respectively, as shown in Fig. 13). The result is

$$K(E_g)=4(C_{11}-C_{12})d\nu, \quad (12a)$$

$$F_3=-(8/\sqrt{3})Pd^2\nu, \quad (12b)$$

where C_{11} and C_{12} are elastic stiffness constants ($C_{11}=3.34\times10^{11}$ and $C_{12}=0.26\times10^{11}$ dyne/cm² at 40°K [18]), d is the ionic distance between Tl^+ and I^- (in this case the K^+-I^- ionic distance of 3.53×10^{-8} cm is used), P is the applied uniaxial stress, ν is a parameter of about unity, and we have assumed that the distortion extends into the effective volume $8d^3\nu$. Then, expressing b in a form involving an unknown parameter t, we can get (without any assumptions on ν)

$$b=-0.9\times10^{-4}/(1-3t^2) \text{ erg/cm}. \quad (13)$$

Though the value of t for the relaxed excited state will differ somewhat from that for the optically excited state, the value of b can be estimated by the use of the latter, which is given as follows:

$$t^2=1/(R+1), \quad (14)$$

where R is the intensity ratio of the A to the C absorption band. The value of t^2 obtained for $R\cong5$, which is estimated from the data of Fukuda *et al.*,[2] is about $\frac{1}{6}$. Using the above value instead of the value of t for the relaxed excited state, we obtain

$$b=-1.8\times10^{-4} \text{ erg/cm}.$$

[18] M. H. Norwood and C. V. Briscoe, Phys. Rev. **112**, 45 (1958).

B. Coupling Constant for T_{2g}-Mode

A uniaxial stress applied in a ⟨110⟩ direction has the following components[17]:

$$P_1=\tfrac{1}{3}P \quad (A_{1g}), \tag{15a}$$

$$P_3=-\tfrac{1}{3}P \quad (E_g), \tag{15b}$$

$$P_6=\tfrac{1}{2}P \quad (T_{2g}). \tag{15c}$$

In this case, the behavior of the excited electronic state under applied stress can be discussed in the (Q_2,Q_3,Q_6) subspace. That is, as $Q_4=Q_5=0$ and $Q_6\neq 0$, $\psi_0{}^z$ continues to be an eigenstate, but $\psi_0{}^x$ and $\psi_0{}^y$ mix with each other as a result of the Q_6 distortion. The solution of the secular equation gives the eigenvalues as

$$E^{\pm}=U_L-(1/\sqrt{3})\beta Q_3\pm(\beta^2Q_2{}^2+\gamma^2Q_6{}^2)^{1/2} -F_3Q_3-F_6Q_6, \tag{16a}$$

$$E^z=U_L+(2/\sqrt{3})\beta Q_3-F_3Q_3-F_6Q_6, \tag{16b}$$

where

$$U_L=\tfrac{1}{2}K(E_g)(Q_2{}^2+Q_3{}^2)+\tfrac{1}{2}K(T_{2g})Q_6{}^2. \tag{17}$$

The electrons will not populate the branch E^+, whose energy is higher than that of branch E^-; thus the luminescence will be due to the transitions from the two minimum points $[{}^0E_{(1)}{}^-, {}^0E_{(2)}{}^-]$ of the branch E^-, and the mimimum point $({}^0E^z)$ of the branch E^z. The Q_3 and Q_6 distortions give the energy difference between ${}^0E^-$ and ${}^0E^z$, and the resulting population difference produces a stress effect on the emission bands. In the case of ⟨110⟩ stress, however, our measurement of the stress effect is not subject to the $\psi_0{}^z$ state, but to the mixtures of $\psi_0{}^x$ and $\psi_0{}^y$. Thus, $I_{\parallel}$ and $I_{\perp}$ relate only to the emission due to transitions from the two minimum points of the E^- branch. The Q_6 distortion does not create an energy difference between the two minima of the E^- state, so the stress effect ($r=I_{\parallel}/I_{\perp}=0.975\neq 1$) on the 336-mμ emission band shown in Fig. 12 cannot be interpreted in terms of the population difference; but it can be understood by the following consideration. Under the Q_6 distortion, the eigenstates are written as

$$|\psi^{(1)\text{ or }(2)}\rangle=a_x{}^-|\psi^x\rangle+a_y{}^-|\psi^y\rangle. \tag{18}$$

The assumption that the value of $|\gamma Q_6|$ produced by the uniaxial stress is much smaller than the value of $|\beta Q_2|$ given by Jahn-Teller distortion simplifies the expression of $a_x{}^-$ and $a_y{}^-$ which are shown in Table II. The intersection of the adiabatic potential surface with the $E^{\pm}$ branches at $Q_3=Q_3{}^0$ and $Q_6=Q_6{}^0$ in the (Q_2,Q_3,Q_6) subspace is shown in Fig. 16 ($\pm Q_2{}^0$, $Q_3{}^0$, and $Q_6{}^0$ are the coordinates of the two minimum poins). Hereafter, we will treat only the A state, where β is positive (because the coupling constant $b<0$). Then in case (1), where luminescence is emitted from ${}^+Q_2{}^0$ configuration, $\beta\,{}^+Q_2{}^0>0$. In case (2), where luminescence is emitted from ${}^-Q_2{}^0$ configuration, $\beta\,{}^-Q_2{}^0<0$. If we assume $\gamma Q_6{}^0$ to be positive (this assumption means that coupling constant $c>0$, because $Q_6{}^0<0$ in this case), eigenfunctions at minimum points $(\psi_0{}^{(1)},\psi_0{}^{(2)})$ are given from

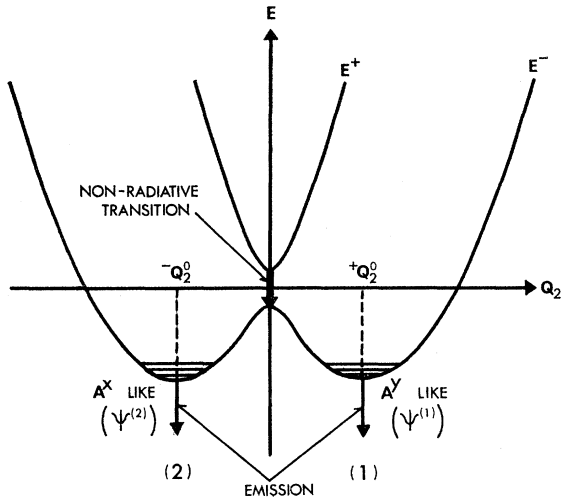

FIG. 16. Intersection of the adiabatic potential surface under ⟨110⟩ stress (at $Q_3=Q_3{}^0$, $Q_6=Q_6{}^0$).

Table II. Making use of these eigenfunctions, the intensity ratio of the ∥ to the ⊥ components of the emissions can be obtained as follows:

$$I_{\parallel}/I_{\perp}=1-2\Delta_0, \tag{19a}$$

where $\Delta_0=(|\gamma Q_6{}^0|/|\beta\,{}^{\pm}Q_2{}^0|)\propto P$, and higher-order terms in Δ_0 are neglected. This result shows that the transition dipoles are rotated by the stress as shown in Fig. 17. Similarly, if $\gamma Q_6{}^0$ is negative, the intensity ratio can be written as

$$I_{\parallel}/I_{\perp}=1+2\Delta_0. \tag{19b}$$

Experimental results indicate $I_{\parallel}<I_{\perp}$, and Δ_0 is always positive; therefore, $\gamma Q_6{}^0>0$, and we can conclude that c is positive. In addition, $I_{\parallel}/I_{\perp}$ can be expressed with β, γ, $K(E_g)$, $K(T_{2g})$, and F_6 as follows:

$$I_{\parallel}/I_{\perp}=1-2|\gamma K(E_g)F_6/[K(T_{2g})\beta^2-K(E_g)\gamma^2]|. \tag{20}$$

The above result, which is independent of temperature, is consistent with the experimental results. The values of β, $K(E_g)$, and d come from Sec. IV A; the values of $K(T_{2g})$ and F_6 are obtained by simple considerations with the help of the definition of the Q_6 expressed by $Y_1=X_2=\tfrac{1}{2}Q_6$ (where Y_1 and X_2 are the displacements of the first and second ligand ions, respectively, as shown in Fig. 13), as follows:

$$K(T_{2g})=16C_{44}d\nu, \tag{21a}$$

$$F_6=-8Pd^2\nu, \tag{21b}$$

where $C_{44}=0.368\times 10^{11}$ dyn/cm² at 40°K,[18] and $8d^3\nu$ is the effective volume into which Q_6 distortion extends.

TABLE II. Mixing coefficients $a_x{}^-$ and $a_y{}^-$ when $\Delta=|\gamma Q_6|/|\beta Q_2|\ll 1$.

	$\gamma Q_6>0$		$\gamma Q_6<0$	
	$\beta Q_2>0$	$\beta Q_2<0$	$\beta Q_2>0$	$\beta Q_2<0$
$a_x{}^-$	$\frac{1}{2}\Delta$	$1-\frac{1}{8}\Delta^2$	$\frac{1}{2}\Delta$	$1-\frac{1}{8}\Delta^2$
$a_y{}^-$	$-1+\frac{1}{8}\Delta^2$	$-\frac{1}{2}\Delta$	$1-\frac{1}{8}\Delta^2$	$\frac{1}{2}\Delta$

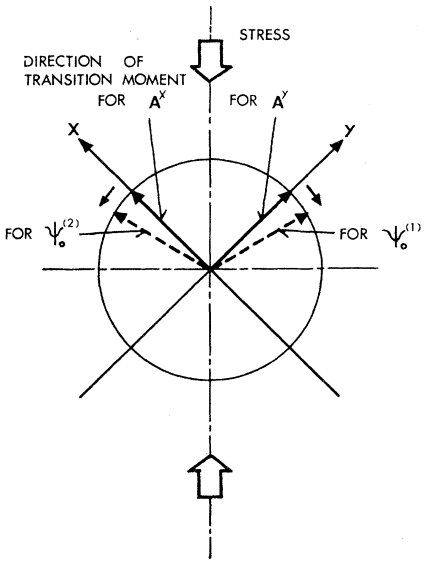

FIG. 17. Rotation of transition moments between the relaxed excited state and ground state due to ⟨110⟩ stress.

Using the value of $I_{\parallel}/I_{\perp}$ $(=0.975)$ and the value of $P(=1.66$ kg/mm$^2)$, the coupling constant c is given as

$$c=0.12\times10^{-4}/(1-3t^2) \text{ erg/cm} \quad \text{(assuming that } \nu=1). \quad (22)$$

Then, if the value of t for the optically excited state $(t^2=\frac{1}{6})$ is used, we get $c=0.24\times10^{-4}$ erg/cm. The values of b and c obtained in the present experiment are not unreasonable in comparison with the results for the optically excited state,[2–4,19] and are consistent with the point-charge model.[3]

V. COMMENTS ON THE 289- AND 430-mμ EMISSION BANDS

Since no stress effect appears in the 289-mμ emission band under ⟨001⟩ and ⟨110⟩ stress, the 272- and 289-mμ bands are not a single emission band split by the reabsorption in the A band, but must have different origins. This is consistent with the conclusions of the methods by Illingworth[10] and Edgerton.[11] An assignment of the 289-mμ emission band to the transitions from the $^3T_{2u}$ and ^3E_u states to the $^1A_{1g}$ state leads to the expectation of a stress effect on the 289-mμ band as well as on the 336-mμ band. As mentioned above, however, the experimental result is contrary to the above expectation. This is an interesting fact. It might relate to the fact that the transition from the $^3T_{2u}$, ^3E_u to $^1A_{1g}$ is induced by the vibrational mixing effect, or it might suggest that the 289-mμ band is related to the nondegenerate state.

Different types of stress effects appear in the 430-mμ band. It seems that the 430-mμ band is not due to a transition related to $^3A_{1u}$, but to one related to the other degenerate electronic state. Qualitatively, the stress effects on 430-mμ band under ⟨001⟩ stress and under ⟨110⟩ stress are similar to the stress effects on the 272-mμ band under ⟨110⟩ stress and under ⟨001⟩ stress, respectively. Therefore, it seems that the transition dipole relating to the 430-mμ band has a component in the [110] or [111] direction. It is not unthinkable that the origin of this emission band is a transition from other stable lattice configuration of $^3T_{1u}$ electronic state by Jahn-Teller effect. At the present stage, however, we cannot say anything conclusive.

VI. CONCLUSION

Useful information on the relaxed excited state of KI:Tl phosphor can be obtained from the stress effect on the 272- and 336-mμ emission bands. In the present work, however, the experiments were carried out mainly on the 336-mμ band, because the observed intensity of the 272-mμ band is weak except at extremely low temperatures. The measurements of the temperature dependence of the stress-induced dichroism on the 336-mμ emission band excited in the A absorption band tell us the following facts:

First, above 35°K, thermal equilibrium exists between the three minimum points of $^3T_{1u}$ state in E_g subspace. As the temperature rises above 35°K, however, the transition from the $^3T_{1u}$ to the excited state related to the 430-mμ emission band increases gradually as a result of phonon processes.

Second, there is no thermal equilibrium below 35°K, because of the existence of potential barriers between the minimum points of $^3T_{1u}$ in E_g subspace. The appearance of the correlation of the polarization of luminescence below 30°K supports this conclusion.

Third, it is concluded from the results below 20°K that there is a small transition probability between the three minimum points even at extremely low temperatures. It seems to be due to the tunnel effect.

Fourth, the behavior of the excited states under ⟨001⟩ and ⟨110⟩ stress was revealed in detail, and the value of the coupling constants was determined. The coupling constants b and c thus obtained, which are negative and positive, respectively, reflect in addition the stress-induced dichroism of the 272-mμ emission band, and are consistent with the point-charge model.

There are some limitations to the analysis for the coupling constants. We have neglected (a) the difference between the mixing coefficient t for the optically excited state and that for the relaxed excited state, (b) dynamical effects due to lattice vibration, and (c) local effects on the elastic constant around the Tl^+ ion. From the above reason, the results obtained here give only an approximate value of the coupling constant for the relaxed excited state.

ACKNOWLEDGMENT

The authors are greatly indebted to Professor T. Yamaguchi of Tottori University for valuable discussions about this work.

[19] D. Bimberg, W. Dultz, and W. Gebhardt, Phys. Status Solidi 31, 661 (1969).